Modeling the ankle articular complex: a computational and experimental analysis

Mariana Rodrigues da Silva[1,2], **Filipe Marques**[1,2], **Sérgio Gonçalves**[3], **Miguel Tavares da Silva**[3], **Paulo Flores**[1,2]

[1] CMEMS-UMinho, Departamento de Engenharia Mecânica, Universidade do Minho, Campus de Azurém, Guimarães, 4804-533, Portugal
[m.silva, fmarques, pflores]@dem.uminho.pt

[2] LABBELS, Associate Laboratory, Braga/Guimarães, Portugal

[3] IDMEC, Instituto Superior Técnico, Universidade de Lisboa, Av. Rovisco Pais, 1, 1049-001, Lisboa Portugal
[sergio.goncalves, miguelsilva]@tecnico.ulisboa.pt

ABSTRACT

Biomechanical models provide information on parameters that are difficult to measure experimentally. The validity of the results depends on the development of anatomically accurate models, including reliable modeling of anatomical articulations. The focus of this work is on the talocrural and talocalcaneal articulations, which collectively form the ankle articular complex of the human foot. Some studies include the talocrural articulation only and formulate it as a revolute joint. Other studies consider both articulations, which are modeled as spherical, revolute, or classical universal joints. Most of the existing approaches do not consider a sufficiently accurate anatomical modelling of this articular complex. Thus, this work presents a new formulation of the ankle articular complex by considering the actual anatomy and movements of the talocrural and talocalcaneal articulations. The proposed approach uses a modified universal joint, incorporated with a massless link that implicitly models the talus bone and mimics its real function. A three-dimensional biomechanical multibody model is used, which is composed of three rigid bodies, namely leg, main foot, and toes. The bodies are kinematically connected to each other by one revolute joint (metatarsophalangeal articulations), and one modified universal joint (ankle articular complex). The model has nine degrees-of-freedom, which are guided using experimental gait data of one adult subject with no history of gait disorders. The formulation developed to guide the degrees-of-freedom of the model is presented. The talocrural and talocalcaneal joint angles, moments of force and mechanical powers are analyzed. The obtained results show good agreement when compared with the literature.

Keywords: Foot model, Ankle articular complex, Modified universal joint, Massless link, Multibody dynamics.

1 INTRODUCTION

The human foot comprises three main bone groups, namely, the tarsus, the metatarsus, and the phalanges, as it can be observed in Figure 1a. The tarsus is composed of seven bones, namely the calcaneus, the talus, the navicular, the cuboid and three cuneiform bones. The metatarsus group includes five metatarsal bones, which are numbered from one to five with roman numerals. Finally, there are two phalanges in the great toe (proximal and distal), while the remaining toes comprise three phalanges each (proximal, middle, and distal) [1] (see Figure 1a). The intricate interconnections established between the bones of the human foot result in 31 articulations that

allow the movements performed during daily life. Amongst these articulations, the talocrural and the talocalcaneal articulations, which collectively form the ankle articular complex of the human foot [2], are the focal point of the present research work. The talocrural articulation enables plantarflexion and dorsiflexion, while the talocalcaneal articulation allows inversion and eversion of the foot [3]. The anatomical axes of these two articulations are non-coplanar and the separating distance can be established as the height of the talus since this bone is inserted between them [4,5]. A schematic representation of the ankle articular complex is depicted in Figure 1b.

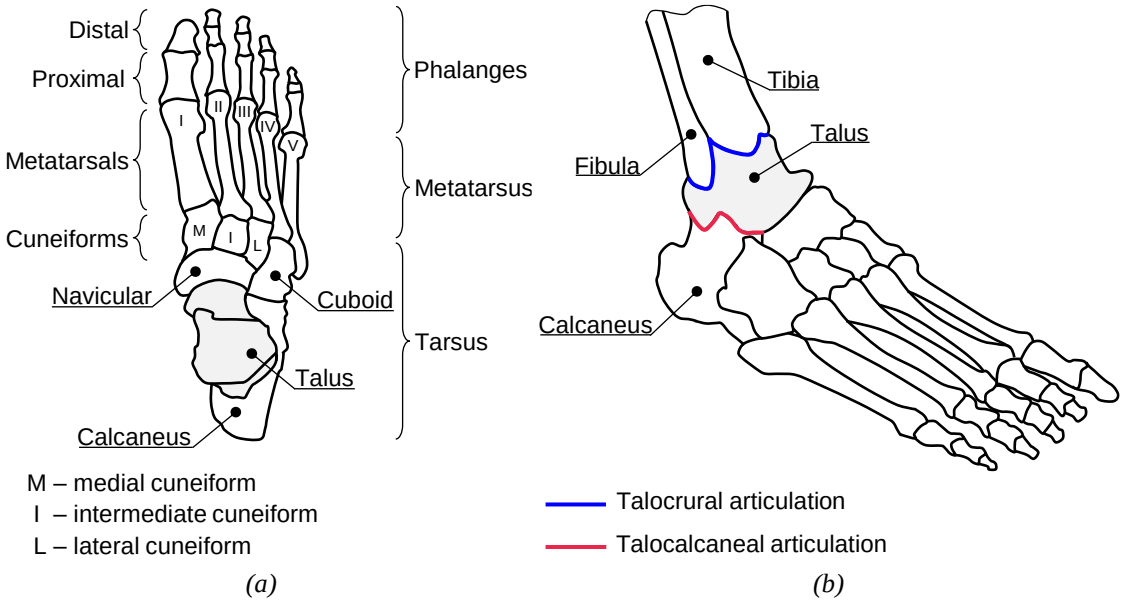

Figure 1. *Schematic representation of the (a) bones and (b) ankle articular complex of the right human foot.*

The human foot and the ankle articular complex can be modeled using different approaches, which present varying degrees of complexity and mimic more or less accurately the anatomical characteristics of the foot [6–10]. Some models consider the dorsiflexion and plantarflexion movements only and formulate the talocrural articulation as an ideal revolute joint, either in two- [11] or three-dimensions [12]. More detailed models consider the movements allowed by both the talocrural and the talocalcaneal articulations. In these cases, the ankle articular complex is modeled as a spherical joint [13], as two [14] or three [15] separate revolute joints, and as a classical universal joint [5]. The available studies have not yet considered a sufficiently anatomically accurate modelling of this articular complex, which plays a key role in studying the movement of the human foot. Thus, this work presents a new formulation of the ankle articular complex of the human foot, which takes into consideration the actual anatomy and movements of the talocrural and talocalcaneal articulations. The proposed approach uses a modified universal joint, which is incorporated with a massless link that implicitly models the talus bone and mimics its real function. A three-dimensional biomechanical multibody model of the right human leg and foot is used. The model has nine degrees-of-freedom, which are guided using gait experimental data of one adult subject with no history of gait disorders acquired at the Lisbon Biomechanics Laboratory. The talocrural and talocalcaneal joint angles, moments of force and mechanical powers are compared with the literature and the response of the proposed joint model is assessed.

2 MULTIBODY SYSTEMS METHODOLOGY

A multibody system includes three main features, that is, rigid and/or deformable bodies describing large rotational and translational displacements, joints that kinematically constrain the relative motion of the adjacent bodies, and force or driving elements. The Newton-Euler approach is amongst the most widely used methods to model multibody systems due to its straightforward application and simplicity [16,17]. The formulation considered in this work uses Cartesian coordinates, in which the degrees-of-freedom of each body of the system are described by three translation (x, y and z) and four orientation coordinates (Euler parameters). The equation of motion for a general constrained multibody system is formulated as [16]

$$\begin{bmatrix} \mathbf{M} & \mathbf{D}^{\mathrm{T}} \\ \mathbf{D} & \mathbf{0} \end{bmatrix} \begin{Bmatrix} \dot{\mathbf{v}} \\ \boldsymbol{\lambda} \end{Bmatrix} = \begin{Bmatrix} \mathbf{g} \\ \boldsymbol{\gamma} \end{Bmatrix} \tag{1}$$

where $\mathbf{M}$ is the system mass matrix, $\mathbf{D}$ represents the Jacobian matrix of the constraint equations, $\dot{\mathbf{v}}$ denotes the vector containing the system accelerations, $\boldsymbol{\lambda}$ is Lagrange multipliers vector that contains the forces and moments associated with the kinematic constraints, $\mathbf{g}$ represents the vector of applied forces and moments, and $\boldsymbol{\gamma}$ denotes the right-hand side vector of the acceleration constraint equations [16,17].

3 FORMULATION TO MODEL THE ANKLE ARTICULAR COMPLEX

In this work, a modified universal joint incorporated with a massless link representing the talus bone is proposed for the ankle articular complex of the human foot (see Figure 2a), which closely follows the work developed by Malaquias et al. [18]. A general representation of the proposed joint model connecting bodies *i* and *j* is depicted in Figure 2b. The centers of mass of the bodies are O_i and O_j, respectively. Body-fixed coordinate systems $\xi\eta\zeta$ are attached to the center of mass, whilst *xyz* represents the global coordinate system.

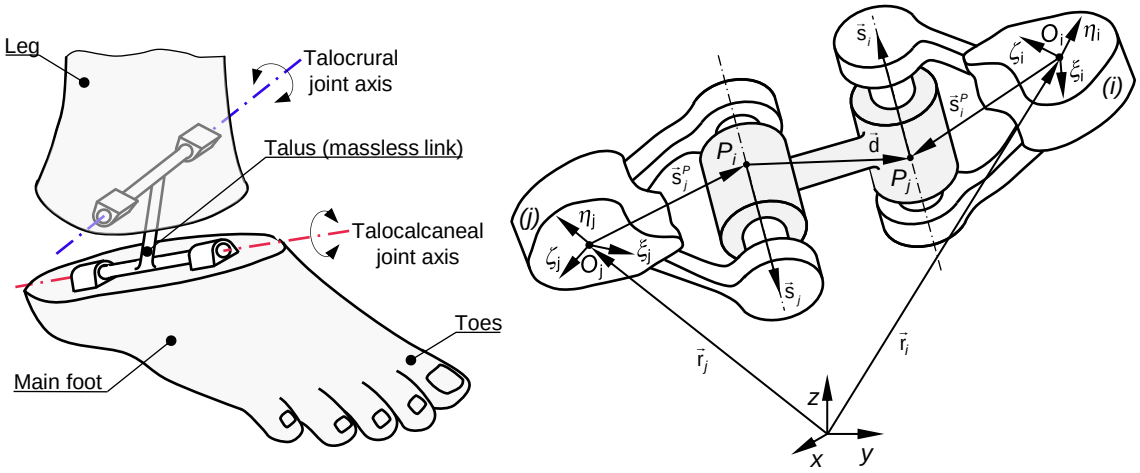

Figure 2. *(a) The ankle articular complex illustrated as a modified universal joint. (b) Schematic representation of a modified universal joint connecting bodies i and j.*

The modified universal joint allows two relative degrees-of-freedom between the connected bodies. Thus, four kinematic constraint equations must be considered to formulate this joint as

$$\boldsymbol{\Phi}^{(\mathrm{u_m},4)} = \begin{cases} \mathbf{d}^{\mathrm{T}}\mathbf{d} - l^2 = 0 \\ \mathbf{s}_i^{\mathrm{T}}\mathbf{s}_j - \mathbf{s}_{i,0}^{\mathrm{T}}\mathbf{s}_{j,0} = 0 \\ \mathbf{s}_i^{\mathrm{T}}\mathbf{d} - \mathbf{s}_{i,0}^{\mathrm{T}}\mathbf{d}_0 = 0 \\ \mathbf{s}_j^{\mathrm{T}}\mathbf{d} - \mathbf{s}_{j,0}^{\mathrm{T}}\mathbf{d}_0 = 0 \end{cases} \tag{2}$$

where $\mathbf{s}_i$ and $\mathbf{s}_j$ represent the vectors of the joint's axes, l denotes the length of the massless link, and $\mathbf{d}$ is established as

$$\mathbf{d} = \mathbf{r}_j^P - \mathbf{r}_i^P = \mathbf{r}_j + \mathbf{s}_j^P - \mathbf{r}_i - \mathbf{s}_i^P \tag{3}$$

in which $\mathbf{r}_k^P$ is the global position vector of point P located on body k (k=i, j), $\mathbf{r}_k$ denotes the position vector of the center of mass of body k described in global coordinates and $\mathbf{s}_k^P$ is the global position vector of point P located on body k with respect to the body's local coordinate system [16]. Vectors $\mathbf{s}_{i,0}$, $\mathbf{s}_{j,0}$ and $\mathbf{d}_0$ denote the initial coordinates of vectors $\mathbf{s}_i$, $\mathbf{s}_j$ and $\mathbf{d}$, respectively.

The first branch of Eq. (2) allows to establish a constant length between points P_i and P_j on each of the joint axes (see Figure 2b), and it represents a link connecting the two bodies, which is not modeled as an actual body, but instead as a massless element. The massless link corresponds to the talus bone of the ankle articular complex. The remaining branches of Eq. (2) allow to maintain the relative orientation of vectors $\mathbf{s}_i$, $\mathbf{s}_j$ and $\mathbf{d}$ constant at all configurations.

The contribution to the Jacobian matrix of the modified universal joint constraints is denoted as

$$\mathbf{D}^{(u_m,4)} = \begin{bmatrix} -2\mathbf{d}^T & 2\mathbf{d}^T\tilde{\mathbf{s}}_i^P & 2\mathbf{d}^T & -2\mathbf{d}^T\tilde{\mathbf{s}}_j^P \\ \mathbf{0} & -\mathbf{s}_j^T\tilde{\mathbf{s}}_i & \mathbf{0} & -\mathbf{s}_i^T\tilde{\mathbf{s}}_j \\ -\mathbf{s}_i^T & -\mathbf{d}^T\tilde{\mathbf{s}}_i + \mathbf{s}_i^T\tilde{\mathbf{s}}_i^P & \mathbf{s}_i^T & -\mathbf{s}_i^T\tilde{\mathbf{s}}_j^P \\ -\mathbf{s}_j^T & \mathbf{s}_j^T\tilde{\mathbf{s}}_i^P & \mathbf{s}_j^T & -\mathbf{d}^T\tilde{\mathbf{s}}_j - \mathbf{s}_j^T\tilde{\mathbf{s}}_j^P \end{bmatrix} \tag{4}$$

Finally, the right-hand side vector of the acceleration constraint equations of the modified universal joint can be established as

$$\boldsymbol{\gamma}^{(u_m,4)} = \begin{Bmatrix} 2\mathbf{d}^T(\tilde{\boldsymbol{\omega}}_i\dot{\mathbf{s}}_i^P - \tilde{\boldsymbol{\omega}}_j\dot{\mathbf{s}}_j^P) - 2\dot{\mathbf{d}}^T\dot{\mathbf{d}} \\ -\mathbf{s}_i^T\tilde{\boldsymbol{\omega}}_j\dot{\mathbf{s}}_j - \mathbf{s}_j^T\tilde{\boldsymbol{\omega}}_i\dot{\mathbf{s}}_i - 2\dot{\mathbf{s}}_j^T\dot{\mathbf{s}}_i \\ -\mathbf{d}^T\tilde{\boldsymbol{\omega}}_i\dot{\mathbf{s}}_i - 2\dot{\mathbf{d}}^T\dot{\mathbf{s}}_i - \mathbf{s}_i^T\tilde{\boldsymbol{\omega}}_j\dot{\mathbf{s}}_j^P + \mathbf{s}_i^T\tilde{\boldsymbol{\omega}}_i\dot{\mathbf{s}}_i^P \\ -\mathbf{d}^T\tilde{\boldsymbol{\omega}}_j\dot{\mathbf{s}}_j - 2\dot{\mathbf{d}}^T\dot{\mathbf{s}}_j - \mathbf{s}_j^T\tilde{\boldsymbol{\omega}}_j\dot{\mathbf{s}}_j^P - \mathbf{s}_j^T\tilde{\boldsymbol{\omega}}_i\dot{\mathbf{s}}_i^P \end{Bmatrix} \tag{5}$$

in which the dot represents the derivative with respect to time, $\boldsymbol{\omega}$ is the angular velocity vector in global coordinates, and the symbol (~) denotes the skew symmetric matrix.

The proposed approach has four major advantages, namely (*i*) the physiological distance between the talocrural and talocalcaneal joints is preserved; (*ii*) the specific anatomical orientation of the joint axes is taken into account; (*iii*) the complexity of the model is not increased as the number of coordinates and constraints is kept unchanged; and (*iv*) the addition of the talus with small mass and inertia in the mass matrix is avoided, which prevents the calculation of high accelerations during the resolution of Eq. (1) and increases the computational efficiency [5,18].

4 DESCRIPTION OF THE CONSIDERED BIOMECHANICAL MODEL

A three-dimensional biomechanical multibody model was developed using an in-house code. The model is composed of three rigid bodies, namely the leg, main foot, and toes. The leg represents the tibia and fibula, the main foot is composed of the tarsus and metatarsus, and the toes encompass the phalanges. The bodies of the model are kinematically connected to each other by means of one revolute joint, connecting the toes to the main foot and representing the metatarsophalangeal articulations, and one modified universal joint, connecting the main foot to the leg and representing the ankle articular complex. Thus, the considered biomechanical model has nine degrees-of-freedom. The generic configuration of the model is displayed in Figure 3.

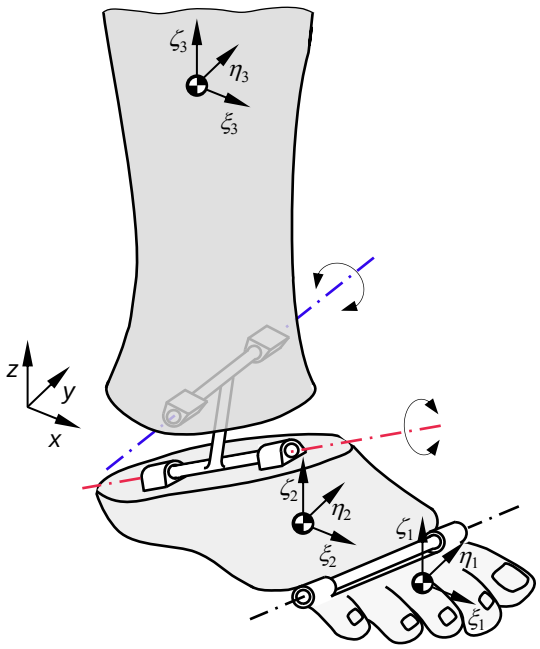

***Figure 3**. Schematic representation of the considered biomechanical multibody model.*

The dimensions and inertial properties of each body of the biomechanical model were calculated using the experimentally acquired data and the anthropometric parameters provided in [5].

5 EXPERIMENTAL ACQUISITION PROTOCOL AND DATA TREATMENT

The experimental gait data of one adult female subject (22 years old, 96.1 kg) with no history of gait disorders was acquired at the Lisbon Biomechanics Laboratory, at *Instituto Superior Técnico*. The laboratory is equipped with an optoelectronic motion capture system, composed of fourteen Infrared ProReflex 1000 cameras (Qualisys©, Göteborg, Sweden) and one video camera (Sony HDR-HC3E). Three force plates (AMTI OR 6-7-1000, 508 mm x 464 mm) were used to acquire the ground reaction forces. The video, markers' positions, ground reaction forces and center of pressure data were acquired synchronously using the Qualisys Track Manager 2.9 (Qualisys©) software. The sampling frequency was set to 100 Hz.

The subject was asked to walk continuously with her natural cadence. Prior to data acquisition, the subject had a period of adaptation to the experimental setup. A 15-second static trial was performed, followed by three valid trials. A trial is considered to be valid if the subject's feet hit correctly the three force plates (one foot per plate) without adapting the cadence or step length.

The marker set protocol utilized in the present work follows the one proposed by Malaquias et al. [18] with some modifications. The protocol is based on the bony landmarks specified on the recommendations of the International Society of Biomechanics [19]. Eleven reflective markers with 11 mm of diameter for the right foot and leg were used during the gait trials. Two markers, M8s and M9s, were used for calibration during static acquisitions only, allowing to define the axis of rotation of the talocalcaneal joint [4]. The midpoints of markers M3 and M4, and M6 and M7 enable the definition of the metatarsophalangeal and talocrural joint axes of rotation, respectively. A cluster of tracking markers was used on the leg to allow the reconstruction of markers M10 and M11. A schematic representation of the marker set protocol is presented in Figure 4.

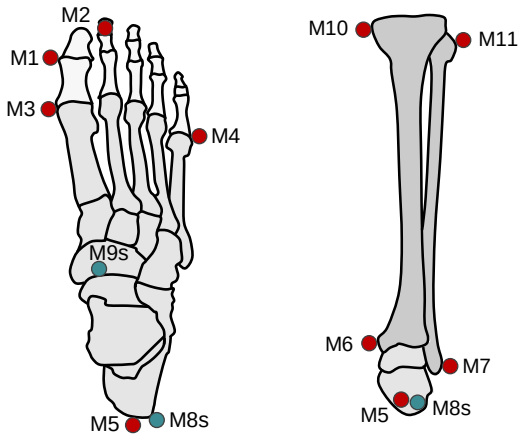

M1 - Medial aspect of the hallux
M2 - Top head of the phalange II
M3 - Medial aspect of the head of metatarsal I
M4 - Lateral aspect of the head of metatarsal V
M5 - Posterior aspect of the calcaneus
M6 - Apex of the medial malleolus
M7 - Apex of the lateral malleolus
M8s - Posterior-lateral "corner" of the heel
M9s - Super-medial aspect of the talus
M10 - Medial apex of the head of the tibia
M11 - Lateral apex of the head of the fibula

***Figure 4**. Marker set protocol considered in the present work.*

A third order low pass digital Butterworth filter with a cutoff frequency of 6 Hz for the kinematic data, 15 Hz for the center of pressure, and 20 Hz for the ground reaction forces was employed. The filtered data was used to calculate the joint angles and the coordinates of the biomechanical model, including the position of the center of mass and the Euler parameters of each segment, which are necessary to prescribe the experimental data to the model.

6 DRIVING CONSTRAINTS FORMULATION

The nine degrees-of-freedom of the biomechanical multibody model presented in Section 4 must be guided. The position of the center of mass and Euler parameters of the leg, and the talocrural, talocalcaneal and metatarsophalangeal joint angles are guided. The formulation used to prescribe the experimental data to the model considers four types of driving constraints, namely guiding (*i*) a generic point *G*, (*ii*) an arbitrary Euler parameter to control the orientation of a body, (*iii*) an angle between two vectors $\mathbf{a}_i$ and $\mathbf{b}_j$ and (*iv*) an angle between a vector $\mathbf{a}_i$ and a massless link **d**.

To guide a generic point *G*, the following three kinematic constraints must be considered

$$\mathbf{\Phi}^{(G,3)} = \mathbf{r}_i^G - \mathbf{c}^*(t) = \mathbf{r}_i + \mathbf{s}_i^G - \mathbf{c}^*(t) = \mathbf{0} \tag{6}$$

where $\mathbf{c}^*(t)$ is the prescribed experimental data containing the *x*, *y*, and *z* coordinates of the guided point and *t* is the time variable.

The corresponding contribution to the Jacobian matrix, the right-hand side contributions of the velocities and acceleration are as

$$\mathbf{D}^{(G,3)} = \begin{bmatrix} \mathbf{I} & -\tilde{\mathbf{s}}_i^G \end{bmatrix} \tag{7}$$

$$\boldsymbol{\nu}^{(G,3)} = -\frac{\partial \boldsymbol{\Phi}^{(G,3)}}{\partial t} = \dot{\mathbf{c}}^*(t) \tag{8}$$

$$\boldsymbol{\gamma}^{(G,3)} = \tilde{\boldsymbol{\omega}}_i \tilde{\mathbf{s}}_i^G \boldsymbol{\omega}_i + \ddot{\mathbf{c}}^*(t) \tag{9}$$

in which **I** represents the identity matrix.

One arbitrary Euler parameter, e_k, with $k = 0, 1, 2, 3$, can be guided using the following constraint equation, the corresponding Jacobian matrix, and the right-hand side vectors of the velocities and accelerations

$$\Phi^{(e_k,1)} = e_k - e_k^*(t) = 0 \tag{10}$$

$$\mathbf{D}^{(e_k,1)} = \begin{bmatrix} \mathbf{0} & \frac{1}{2}\left(\mathbf{G}_{(1:3,k+1)}\right)^{\mathrm{T}} \end{bmatrix} \tag{11}$$

$$\nu^{(e_k,1)} = -\frac{\partial \boldsymbol{\Phi}^{(e_k,1)}}{\partial t} = \dot{e}_k^*(t) \tag{12}$$

$$\gamma^{(e_k,1)} = \ddot{e}_k^*(t) - \frac{1}{2}\boldsymbol{\omega}_i^{\mathrm{T}} \dot{\mathbf{G}}_{(1:3,k+1)} \tag{13}$$

where $e_k^*(t)$ is the experimental data for e_k and **G** represents the transformation matrix in terms of the Euler parameters [16].

To guide the angle between two arbitrary $\mathbf{a}_i$ and $\mathbf{b}_j$ vectors, each belonging to a body of the multibody system, the following constraint equation must be formulated

$$\Phi^{(\theta,1)} = \mathbf{a}_i^{\mathrm{T}} \mathbf{b}_j - \cos\theta(t) = 0 \tag{14}$$

in which $\theta(t)$ is the angle between the two $\mathbf{a}_i$ and $\mathbf{b}_j$ vectors calculated using the experimental data. It must be noted that $\mathbf{a}_i$ and $\mathbf{b}_j$ must be unit vectors perpendicular to the joint axis. The contribution to the Jacobian matrix, the right-hand side vectors of the velocities and accelerations are as

$$\mathbf{D}^{(\theta,1)} = \begin{bmatrix} \mathbf{0} & -\mathbf{b}_j^{\mathrm{T}} \tilde{\mathbf{a}}_i & \mathbf{0} & -\mathbf{a}_i^{\mathrm{T}} \tilde{\mathbf{b}}_j \end{bmatrix} \tag{15}$$

$$\nu^{(\theta,1)} = -\frac{\partial \boldsymbol{\Phi}^{(\mathbf{s}_i \mathbf{s}_m,1)}}{\partial t} = -\sin\theta(t)\dot{\theta}(t) \tag{16}$$

$$\gamma^{(\theta,1)} = -\mathbf{b}_j^{\mathrm{T}} \tilde{\boldsymbol{\omega}}_i \dot{\mathbf{a}}_i - \mathbf{a}_i^{\mathrm{T}} \tilde{\boldsymbol{\omega}}_j \dot{\mathbf{b}}_j - 2\dot{\mathbf{a}}_i^{\mathrm{T}} \dot{\mathbf{b}}_j - \cos\theta(t)\dot{\theta}(t)^2 - \sin\theta(t)\ddot{\theta}(t) \tag{17}$$

Finally, the last driving constraint is used to guide the angle of each joint of the modified universal joint. To correctly calculate the joint angle, it must be noted that the massless link vector must be projected onto the plane perpendicular to the joint axis. Thus, vector $\mathbf{d}_\mathrm{p}$ is defined as

$$\mathbf{d}_\mathrm{p} = \mathbf{d} - \left(\mathbf{d}^{\mathrm{T}} \mathbf{s}_i\right)\mathbf{s}_i \tag{18}$$

where $\mathbf{s}_i$ is the vector defining the rotation axis of the joint which angle is meant to be guided.

Thus, the kinematic constraint equation used to guide the angle between one arbitrary unit vector $\mathbf{a}_i$ perpendicular to the $\mathbf{s}_i$ joint axis and the projected massless link $\mathbf{d}_\mathrm{p}$ is established as

$$\Phi^{(\beta,1)} = \frac{\mathbf{a}_i^{\mathrm{T}} \mathbf{d}_\mathrm{p}}{\left\|\mathbf{d}_\mathrm{p}\right\|} - \cos\beta(t) = 0 \tag{19}$$

in which $\beta(t)$ is the angle between the $\mathbf{a}_i$ and $\mathbf{d}_\mathrm{p}$ vectors calculated using the experimental data.

The corresponding contribution to the Jacobian matrix and the right-hand side vectors of the velocities and accelerations can be expressed as

$$\mathbf{D}^{(\beta,1)} = \begin{bmatrix} \dfrac{\mathbf{a}_i^{\mathrm{T}}\left(\mathbf{s}_i\mathbf{s}_i^{\mathrm{T}} - \mathbf{I}\right)}{\left\|\mathbf{d}_\mathrm{p}\right\|} & \dfrac{-\mathbf{d}_\mathrm{p}^{\mathrm{T}}\tilde{\mathbf{a}}_i + \mathbf{a}_i^{\mathrm{T}}\left(\tilde{\mathbf{s}}_i^P - \mathbf{s}_i\mathbf{s}_i^{\mathrm{T}}\tilde{\mathbf{s}}_i^P + \mathbf{s}_i\mathbf{d}^{\mathrm{T}}\tilde{\mathbf{s}}_i + \mathbf{d}^{\mathrm{T}}\mathbf{s}_i\tilde{\mathbf{s}}_i\right)}{\left\|\mathbf{d}_\mathrm{p}\right\|} & \dfrac{\mathbf{a}_i^{\mathrm{T}}\left(\mathbf{I} - \mathbf{s}_i\mathbf{s}_i^{\mathrm{T}}\right)}{\left\|\mathbf{d}_\mathrm{p}\right\|} & \dfrac{\mathbf{a}_i^{\mathrm{T}}\left(\mathbf{s}_i\mathbf{s}_i^{\mathrm{T}}\tilde{\mathbf{s}}_j^P - \tilde{\mathbf{s}}_j^P\right)}{\left\|\mathbf{d}_\mathrm{p}\right\|} \end{bmatrix} \tag{20}$$

$$\nu^{(\beta,1)} = -\frac{\partial \mathbf{\Phi}^{(\beta,1)}}{\partial t} = -\sin\beta(t)\dot{\beta}(t) \tag{21}$$

$$\begin{aligned}\gamma^{(\beta,1)} = \; & \frac{1}{\|\mathbf{d}_{\mathrm{p}}\|}\Big(-\mathbf{d}_{\mathrm{p}}^{\mathrm{T}}\tilde{\boldsymbol{\omega}}_i\dot{\mathbf{a}}_i - 2\dot{\mathbf{d}}_{\mathrm{p}}^{\mathrm{T}}\dot{\mathbf{a}}_i + \mathbf{a}_i^{\mathrm{T}}\left(-\tilde{\boldsymbol{\omega}}_j\dot{\mathbf{s}}_j^P + \tilde{\boldsymbol{\omega}}_i\dot{\mathbf{s}}_i^P + \dot{\mathbf{d}}^{\mathrm{T}}\dot{\mathbf{s}}_i\mathbf{s}_i + \mathbf{s}_i^{\mathrm{T}}\tilde{\boldsymbol{\omega}}_j\dot{\mathbf{s}}_j^P\mathbf{s}_i\right.\right. \\ & \left.\left. -\mathbf{s}_i^{\mathrm{T}}\tilde{\boldsymbol{\omega}}_i\dot{\mathbf{s}}_i^P\mathbf{s}_i + \mathbf{s}_i^{\mathrm{T}}\dot{\mathbf{d}}\dot{\mathbf{s}}_i + \dot{\mathbf{s}}_i^{\mathrm{T}}\dot{\mathbf{d}}\mathbf{s}_i + \mathbf{d}^{\mathrm{T}}\tilde{\boldsymbol{\omega}}_i\dot{\mathbf{s}}_i\mathbf{s}_i + 2\mathbf{d}^{\mathrm{T}}\dot{\mathbf{s}}_i\dot{\mathbf{s}}_i + \mathbf{s}_i^{\mathrm{T}}\dot{\mathbf{d}}\dot{\mathbf{s}}_i + \mathbf{d}^{\mathrm{T}}\mathbf{s}_i\tilde{\boldsymbol{\omega}}_i\dot{\mathbf{s}}_i\right)\right) \\ & -\cos\beta(t)\dot{\beta}(t)^2 - \sin\beta(t)\ddot{\beta}(t)\end{aligned} \tag{22}$$

in which the first time derivative of vector $\mathbf{d}_{\mathrm{p}}$ is established as

$$\dot{\mathbf{d}}_{\mathrm{p}} = \dot{\mathbf{d}} - \mathbf{s}_i^{\mathrm{T}}\dot{\mathbf{d}}\mathbf{s}_i - \mathbf{d}^{\mathrm{T}}\dot{\mathbf{s}}_i\mathbf{s}_i - \mathbf{d}^{\mathrm{T}}\mathbf{s}_i\dot{\mathbf{s}}_i \tag{23}$$

7 RESULTS AND DISCUSSION

Since the focus of this work is to propose a new formulation for the ankle articular complex of the human foot, only the results concerning the talocrural and talocalcaneal joints are object of investigation in this Section. The results are presented using the mean and the standard deviation.

The angle and moments of force for the talocrural and for the talocalcaneal joints during the gait cycle are depicted in Figure 5. In general, the profile and magnitude of the talocrural joint angle show good agreement with the results reported in the literature [18,20–22] (see Figure 5a). It is clear that Figure 5a presents the two characteristics loading and unloading phases that occur in human gait, which correspond to the two plantarflexion peaks observed at 10% and 65% of gait cycle, respectively. At the initial support phase (0-10% of gait cycle), the talocrural joint plantarflexes in order to lower the foot towards the ground. When the foot is flat on the ground, the leg starts rotating forward over the foot, provoking dorsiflexion of the talocrural joint (10-50% of gait cycle). Before the toe-off, which occurs at approximately 63% of gait cycle, the talocrural joint plantarflexes, corresponding to the pre-swing phase. During the swing phase of gait, the talocrural joint dorsiflexes in order to prepare the foot for the subsequent gait cycle.

The profile and magnitude of the talocrural joint moment of force is consistent with the literature [18,20–22] (see Figure 5c). In the beginning of the gait cycle, a small dorsiflexion moment is generated to control the lowering of the foot to the ground. Then, from 5% to 50% of gait cycle, there is a large plantarflexion moment to control the forward progression of the leg over the foot, which is flat on the ground. Prior to the toe-off, the talocrural joint moment of force decreases since the corresponding lower limb is being unloaded to prepare for the toe-off. During the swing phase of the gait cycle, since no ground reaction forces are acting on the foot, there is a small dorsiflexion moment to maintain the talocrural joint dorsiflexed, preventing the toes from touching the ground and ensuring a safe toe clearance.

From 0% to 55% of gait cycle, the talocalcaneal joint angle is similar to the results presented in the literature [22–24], both in magnitude and profile of the plot (see Figure 5b). However, from 55% to the end of the gait cycle, the results are different, specifically for the magnitude of the plot. The results show that there is an excessive eversion of the foot prior to the toe-off. According to the literature, the magnitude of the talocalcaneal joint angle should vary between -10º and 10º, as opposed to -25º and 10º shown in Figure 5b. The differences between the results of the present work and the literature might be associated with the specific gait pattern of the considered subject. During experimental data acquisition, excessive eversion of the subject's foot was noticeable, which supports the obtained results. Thus, it can be concluded that the proposed joint model can correctly reproduce the movements of the talocalcaneal joint.

The profile and magnitude of the talocalcaneal joint moment of force (see Figure 5d) agree with the literature [22–24]. In the beginning of the gait cycle, a small eversion moment is generated, followed by a large inversion moment, seen during the majority of the stance phase. Before the toe-off, the moment gradually increases, ultimately reaching a value near zero, which is observed during the swing phase. It is important to mention that the intra-subject variability is greater for the talocalcaneal joint when compared with the talocrural joint due to higher standard deviations.

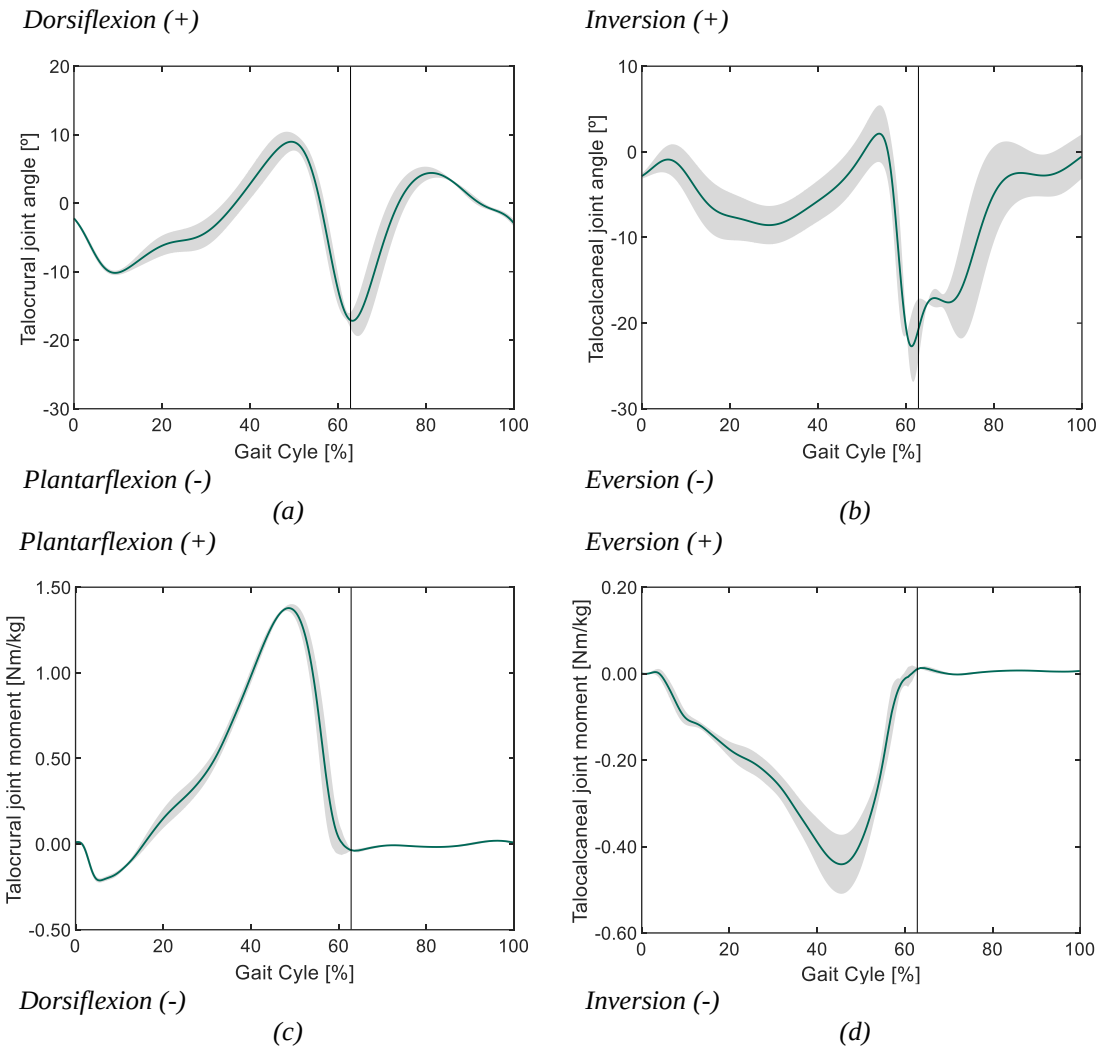

***Figure 5**. Talocrural and talocalcaneal joint angle (a), (b), and moments of force (c), (d) throughout the gait cycle. The black vertical line indicates the occurrence of the toe off.*

The path of the center of pressure is shown in Figure 6. The talocalcaneal joint moment discussed in the above paragraph is consistent with the location of the center of pressure for the considered subject. This can be concluded from the fact that the center of pressure is deviated towards the lateral side of the foot (see Figure 6), provoking an eversion moment on the foot, which must be compensated by an inversion moment (see Figure 5d). The kinematic pattern for the talocalcaneal joint is highly variable and dependent on the type of gait pattern of the subject and the contact of the foot with the ground. Thus, the results for this joint might not represent a generic case.

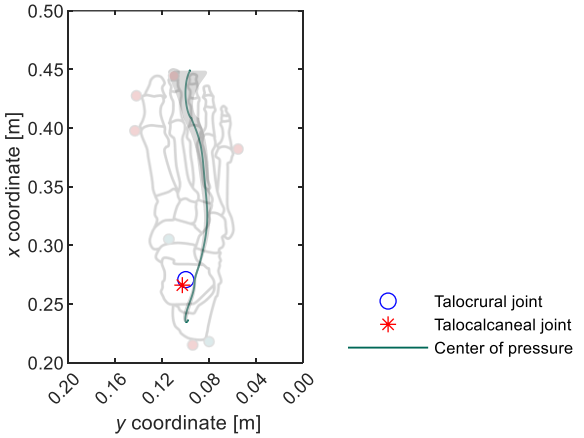

***Figure 6**. Path of the center of pressure from heel contact to toe off.*

The mechanical power is related to the net rate of generating and absorbing energy by the muscles and other tissues crossing a joint. Positive values indicate power generation and concentric muscle activation, while negative values imply power absorption and eccentric muscle activation [20].

The talocrural and the talocalcaneal joint mechanical power is presented in Figure 7. The negative peak observed in the mechanical power plot of the talocrural joint from 0% to 15% of gait cycle indicates that there is power absorption just after heel strike from the muscles responsible for dorsiflexion, which contract eccentrically to control the initial plantarflexion of this joint. Then, from 15% to 50% of the gait cycle, the power absorption increases as the muscles responsible for plantarflexion contract eccentrically during the forward progression of the leg over the foot, indicating an action of the plantarflexors to control the dorsiflexion movement. The maximum positive power magnitude for the talocrural joint occurs at around 55% of the gait cycle, which corresponds to the phase in which the lower limb propels the body forward in preparation for the toe-off and the plantarflexors contract concentrically (see Figure 7a). The results agree with the literature [18,20]. For the talocalcaneal joint, in the beginning of the gait cycle there is power absorption, followed by power generation with a maximum magnitude occurring at around 50% of gait cycle, which agrees with the literature in magnitude and profile of the plot [23,24]. Before the toe off, power absorption occurs with a maximum magnitude of -0.60 W/kg (see Figure 7b), which differs from literature [23,24]. This phenomenon indicates that there is excessive action of the muscles responsible for ankle stabilization due to the high eversion of the foot and it may be related to the differences previously reported for the talocalcaneal joint angle and moment.

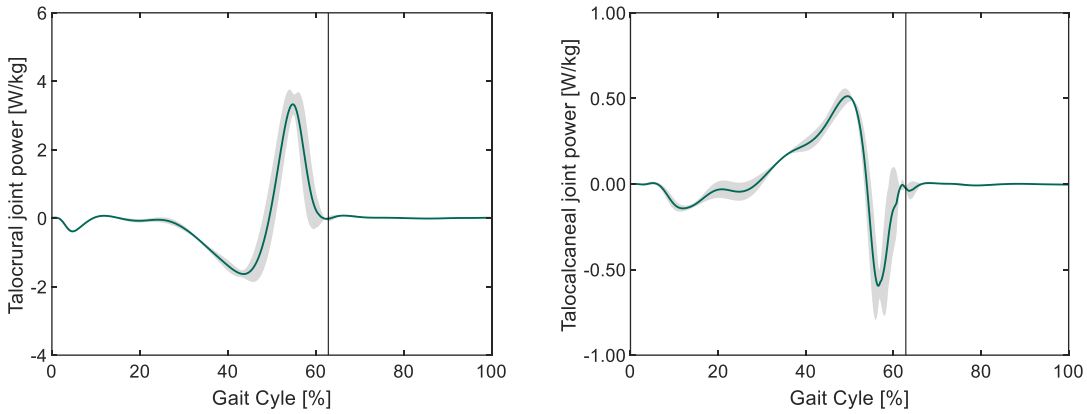

***Figure** 7. Mechanical power of the (a) talocrural and (c) talocalcaneal joints throughout the gait cycle. The black vertical line indicates the occurrence of the toe off.*

A limitation of the present work is that only one subject was considered in the analysis. Future studies should aim at increasing the sample size to evaluate the reliability of the model. However, the obtained results allow the validation of both the proposed joint formulation and the methodology used to prescribe the experimental data to the biomechanical model. The proposed formulation is able to correctly describe the degrees-of-freedom allowed by the ankle articular complex of the human foot, as it could reproduce the biomechanical parameters analyzed in this work according both with the literature and the movements observed during the experimental data acquisition. In addition, the model can realistically represent the anatomical characteristics intrinsic to the human foot due to the fact that the talus bone is modelled implicitly, which allows to preserve the physiological distance between the talocrural and talocalcaneal joints. The specific anatomical orientation of each joint axis is also guaranteed by the model. Finally, even though the proposed formulation is developed using Cartesian coordinates, it can easily be adapted to other multibody formulations, including natural [25] and fully Cartesian [26] coordinates.

8 CONCLUSIONS

In this work, a new formulation to model the ankle articular complex of the human foot has been proposed within the framework of multibody systems methodologies. The main kinematic aspects were described, including the kinematic constraints, Jacobian matrix, and right-hand side vector of the accelerations constraint equations. The degrees-of-freedom of a biomechanical model of the right human foot and leg were guided using experimental gait data. The talocrural and the talocalcaneal joint angles, moments of force and mechanical power showed good agreement with literature. The proposed formulation can correctly reproduce the movements of both articulations.

ACKNOWLEDGMENTS

This work has been supported by Portuguese Foundation for Science and Technology, under the national support to R&D units grant, with the reference project UIDB/04436/2020 and UIDP/04436/2020, as well as through IDMEC, under LAETA, project UIDB/50022/2020. The first author expresses her gratitude to the Portuguese Foundation for Science and Technology through the PhD grant (2021.04840.BD).

REFERENCES

[1] N. Palastanga, R. Soames, Anatomy and human movement: structure and function, Sixth Ed., Elsevier Health Sciences, (2012) ISBN: 978-0-7020-3553-1.
[2] M. Fukano, T. Fukubayashi, S. Banks, Sex differences in three-dimensional talocrural and subtalar joint kinematics during stance phase in healthy young adults, Hum Mov Sci. 61 (2018) 117–125.
[3] B. Pereira, R. Andrade, J. Espregueira-Mendes, R. Marano, X. Oliva, J. Karlsson, Current Concepts on Subtalar Instability, Orthop J Sports Med. 9 (2021) 232596712110213.
[4] R. Isman, V. Inman, Anthropometric studies of the human foot and ankle, Bull Prosthet Res. (1969) 11-14.
[5] F. Anderson, M. Pandy, A Dynamic Optimization Solution for Vertical Jumping in Three Dimensions, Comput Methods Biomech Biomed Engin. 2 (1999) 201–231.
[6] I. Roupa, M.R. Silva, F. Marques, S.B. Gonçalves, P. Flores, M.T. Silva, On the Modeling of Biomechanical Systems for Human Movement Analysis: A Narrative Review, Arch. Comput. Methods Eng. 29 (2022) 4915–4958.
[7] M. Silva, B. Freitas, R. Andrade, Ó. Carvalho, D. Renjewski, P. Flores, J. Espregueira-Mendes, Current Perspectives on the Biomechanical Modelling of the Human Lower Limb: A Systematic Review, Arch. Comput. Methods Eng. 28 (2021) 601–636.
[8] M.R. Silva, F. Marques, M.T. Silva, P. Flores, A Comprehensive Review on Biomechanical Modeling Applied to Device-Assisted Locomotion, Arch. Comput. Methods Eng. 30 (2023) 1897–1960.
[9] L. Saraiva, M.R. Silva, F. Marques, M.T. Silva, P. Flores, A review on foot-ground contact modeling strategies for human motion analysis, Mech Mach Theory. 177 (2022) 105046.
[10] K. Deschamps, F. Staes, P. Roosen, F. Nobels, K. Desloovere, H. Bruyninckx, G.A. Matricali, Body of evidence supporting the clinical use of 3D multisegment foot models: A systematic review, Gait Posture. 33 (2011) 338–349.
[11] M. Shourijeh, J. McPhee, Foot–ground contact modeling within human gait simulations: from Kelvin–Voigt to hyper-volumetric models, Multibody Syst Dyn. 35 (2015) 393–407.
[12] D. Lopes, R. Neptune, J. Ambrósio, M.T. Silva, A superellipsoid-plane model for simulating foot-ground contact during human gait, Comput Methods Biomech Biomed Engin. 19 (2016) 954–963.
[13] F. Mouzo, U. Lugris, R. Pamies-Vila, J. Cuadrado, Skeletal-level control-based forward dynamic analysis of acquired healthy and assisted gait motion, Multibody Syst Dyn. 44 (2018) 1–29.
[14] N. Maniar, A. Schache, C. Pizzolato, D. Opar, Muscle function during single leg landing, Sci Rep. 12 (2022) 11486.
[15] T. Guess, A. Stylianou, M. Kia, Concurrent Prediction of Muscle and Tibiofemoral Contact Forces During Treadmill Gait, J Biomech Eng. 136 (2014) 021032.
[16] P. Nikravesh, Computer-aided analysis of mechanical systems, Prentice-Hall, Inc., (1988) ISBN: 978-0131642201.
[17] M.R. Silva, F. Marques, M.T. Silva, P. Flores, A comparison of spherical joint models in the dynamic analysis of rigid mechanical systems: ideal, dry, hydrodynamic and bushing approaches, Multibody Syst Dyn. 56 (2022) 221–266.
[18] T.M. Malaquias, S.B. Gonçalves, M.T. Silva, A Three-Dimensional Multibody Model of the Human Ankle-Foot Complex, in: P. Flores, F. Viadero (Eds.), New Trends in Mechanism and Machine Science. Mechanisms and Machine Science, Vol. 24, Springer, Cham, (2015): pp. 445–453.
[19] G. Wu, S. Siegler, P. Allard, C. Kirtley, A. Leardini, D. Rosenbaum, M. Whittle, D.D. D'Lima, L. Cristofolini, H. Witte, O. Schmid, I. Stokes, ISB recommendation on definitions of joint coordinate system of various joints for the reporting of human joint motion—part I: ankle, hip, and spine, J Biomech. 35 (2002) 543–548.
[20] D. Neumann, Kinesiology of the Musculoskeletal System: Foundations for Rehabilitation, Second Ed., Mosby - Elsevier, (2010) ISBN: 978-0-323-03989-5.
[21] D. Winter, Biomechanics and Motor Control of Human Movement, Fourth Ed., John Wiley, New York, NY, (1990) ISBN: 978-0-470-39818-0.
[22] S. Scott, D. Winter, Talocrural and talocalcaneal joint kinematics and kinetics during the stance phase of walking, J Biomech. 24 (1991) 743–752.
[23] J. Maharaj, L. Murry, A. Cresswell, G. Lichtwark, Increasing step width reduces the requirements for subtalar joint moments and powers, J Biomech. 92 (2019) 29–34.
[24] J. Maharaj, A. Cresswell, G. Lichtwark, Subtalar Joint Pronation and Energy Absorption Requirements During Walking are Related to Tibialis Posterior Tendinous Tissue Strain, Sci Rep. 7 (2017) 17958.
[25] de Jalón, J. G., Bayo, E., Kinematic and Dynamic Simulation of Multibody Systems: The Real-Time Challenge, Springer-Verlag, New York, NY, (1994) ISBN: 3-540-94096-0.
[26] I. Roupa, S.B. Gonçalves, M.T. Silva, Kinematics and dynamics of planar multibody systems with fully Cartesian coordinates and a generic rigid body, Mech Mach Theory. 180 (2023) 105134.